

Supporting Information

Morphology-Dependent Nanoplasmonic Assay: A Powerful Signaling Platform for Multiplexed Total Antioxidant Capacity Analysis

Zeinab Feyzollahi, Mahdiye Hassanpoor, Afsaneh Orouji, and Mohammad Reza Hormozi-Nezhad *

Department of Chemistry, Sharif University of Technology, Tehran, 111559516, Iran

*Corresponding authors:

- Mohammad Reza Hormozi-Nezhad, email: hormozi@sharif.edu
ORCID iD: 0000-0002-7472-1850

Table of Contents

Content	Page
Chemicals and Materials	S4
Instrumentation	S4
Synthesis of AuNRs	S4
Statistical Analysis	S5
LOD and LOQ Formulas	S6
Fig. S1 Assessing the stability of AuNRs in pH 7 B.R. buffer: UV-vis spectra within 15 minutes.	S7
Table S1. Comparative redox potentials for key antioxidants in the human body.	S8
Fig. S2 Effect of NBS concentrations on the multi-colorimetric responses of AuNRs, (A) the corresponding images of the probe, (B) the absorption spectra of the proposed probe, and (C) the corresponding bar plot as a function of NBS concentration (pH 7 B.R. buffer) at 15 min in both incubation time and analysis time.	S9
Fig. S3 Effect of incubation time on the multi-colorimetric responses of AuNRs, spectral variations of 10 μM of each antioxidant, pH 7 B.R buffer, and analysis time 15 min (A) AA, (B) CYS, (C) GSH, and (D) UA, (E-H) bar plots representing variations of AuNRs spectra as a function of incubation time in the presence of AA, CYS, GSH, and UA respectively.	S10
Fig. S4 UV-vis absorption profile of the proposed probe after 10-minute incubation with 75 μM NBS and 10 μM of individual antioxidants in pH 7 B.R. buffer.	S11
Fig. S5 Effect of time-course variation in absorption spectra of the AuNRs, (A) spectral variations, (B) bar plot representing variations of AuNRs spectra as a function of time-course variation in the presence of 75 μM NBS. The incubation time was 10 min.	S12
Fig. S6 Effect of time-course variation in absorption spectra of the AuNRs, spectral variations of (A) AA, (B) CYS, (C) GSH, and (D) UA, (E-H) bar plots AA variations of AuNRs spectra as a function of time-course variation in the presence of AA, CYS, GSH, and UA, respectively. The concentration of NBS and each antioxidant was 75 $\mu\text{mol L}^{-1}$ and 10 $\mu\text{mol L}^{-1}$, respectively. The incubation time was 10 minutes in pH 7 B.R. buffer.	S13
Fig. S7 (A) Color variation images and variation responses of the probe to different concentrations of (B) AA, (C) CYS, (D) GSH, and (E) UA.	S14
Fig. S8 3D LDA score plots for the discrimination of four classes of antioxidants (i.e., AA, CYS, GSH, and UA) and total antioxidants as a TAC-mixture.	S15
Table S2. Jackknifed classification matrix for the discrimination of single-component samples (AA and CYS 1-60 $\mu\text{mol L}^{-1}$; UA and GSH 0.05-20 $\mu\text{mol L}^{-1}$) and TAC as a multi-component (0.05-14 $\mu\text{mol L}^{-1}$) in their entire concentration range.	S16
Table S3. Jackknifed classification matrix for the discrimination of AA in the entire concentration range.	S17

Table S4. Jackknifed classification matrix for the discrimination of CYS in the entire concentration range. **S18**

Table S5. Jackknifed classification matrix for the discrimination of GSH in the entire concentration range. **S19**

Table S6. Jackknifed classification matrix for the discrimination of UA in the entire concentration range. **S20**

Table S7. Jackknifed classification matrix for the discrimination of TAC in the entire concentration range. **S21**

Fig. S9 Predicted vs measured concentration plots with PLSR for (A) AA, (B) CYS, (C) GSH, (D) and UA. **S22**

Table S8. Comparison of the proposed method with other reported methods for detection of antioxidants. **S23**

Fig. S10 UV-vis spectra and corresponding color photographs of three different TAC unknown in total concentration of 5, 7, and 9 $\mu\text{mol L}^{-1}$ in human saliva sample. **S24**

Table S9. LDA posterior probability outcomes for identifying TAC unknown samples in human saliva. All 9 samples were given as a test set to the pre-trained LDA model of AA, CYS, GSH, UA, and TAC-mixture. **S25**

Table S10. LDA posterior probability outcomes for identifying TAC unknown samples in human saliva. All 9 samples were given as a test set to the pre-trained LDA model of TAC-mixture within the total concentration range of 0.05–14 $\mu\text{mol L}^{-1}$. **S26**

Fig. S11 3D LDA score plots for the discrimination of TAC unknown of real human saliva samples after combining the test set (real samples) with the pre-trained LDA model of AA, CYS, GSH, UA, and TAC-mixture. The saliva samples were spiked with three concentrations of total antioxidant. **S27**

Fig. S12 2D LDA score plots for the discrimination of TAC unknown of real human saliva samples after combining the test set (real samples) with the pre-trained LDA model of TAC-mixture within the total concentration range of 0.05–14 $\mu\text{mol L}^{-1}$. The saliva samples were spiked with three concentrations of total antioxidants. **S28**

Fig. S13 Interference effect on the responses of the proposed probe ($[\text{AA}] = [\text{CYS}] = [\text{GSH}] = [\text{UA}] = [\text{TAC}] = 10 \mu\text{M}$, $[\text{Urea}] = 475 \mu\text{M}$, $([\text{Na}^+] = 1000 \mu\text{M}$, $[\text{Ca}^{2+}] = [\text{K}^+] = 500 \mu\text{M}$, $[\text{Mg}^{2+}] = 650 \mu\text{M}$) ($[\text{Cl}^-] = 650 \mu\text{M}$, $[\text{PO}_4^{3-}] = 375 \mu\text{M}$). **S29**

References **S30**

Chemicals and Materials

Hydrogen tetrachloroaurate ($\text{HAuCl}_4 \cdot 3\text{H}_2\text{O}$) (99.5% w/w), sodium borohydride (NaBH_4), cetyltrimethylammonium bromide (CTAB), ascorbic acid (AA), silver nitrate (AgNO_3), sodium hydroxide (NaOH), ortho-phosphoric acid (85%), acetic acid (glacial) (100%), boric acid, sodium borohydride, sodium hydroxide, and N-bromosuccinimide (NBS), cysteine ($\text{C}_3\text{H}_7\text{NO}_2\text{S}$), glutathione ($\text{C}_{10}\text{H}_{17}\text{N}_3\text{O}_6\text{S}$), and uric acid ($\text{C}_5\text{H}_4\text{N}_4\text{O}_3$) were acquired from Sigma-Aldrich at analytical grade and used without further purification. Milli-Q grade water with a resistivity of 18.2 M Ω was used throughout all experimental procedures in this research.

Instrumentation

Spectrophotometric absorbance measurements were conducted using an Agilent Cary 60 spectrophotometer with 1.0 cm glass cuvettes. Images capturing color variations were taken with a Samsung A71 smartphone. Transmission electron microscopy (TEM) analysis was performed on a Zeiss EM900 microscope, operating at an acceleration voltage of 200 kV. The pH measurements and adjustments to the solutions were carried out using a Denver Instrument Model 270 pH meter equipped with a glass electrode.

Synthesis of AuNRs

AuNRs were synthesized via a seed-mediated growth method, following previously reported protocols¹. The synthesis process involved two main steps: preparing the seed and growth solutions. For the seed solution, 0.125 mL of HAuCl_4 (0.01 mol L⁻¹) and 5.0 mL of CTAB (0.1 mol L⁻¹) were combined, followed by the addition of 0.3 mL of freshly prepared ice-cold NaBH_4 (0.01 mol L⁻¹). This resulted in a brownish-yellow solution, which was allowed to stand at room temperature for 2–5 hours. The growth solution was prepared by mixing 50.0 mL of CTAB (0.1 mol L⁻¹), 2.5 mL of HAuCl_4 (0.01 mol L⁻¹), and 0.3 mL of AgNO_3 (0.01 mol L⁻¹), followed by the addition of 0.3 mL of AA (0.1 mol L⁻¹). The color change from yellow to colorless indicated the reduction of Au^{3+} to Au^+ . Finally, the 0.25 mL seed solution was gently added to the growth mixture, and then left overnight at room temperature. Excess CTAB was eliminated through centrifugation at 8000 rpm for 15 minutes, and the AuNRs were isolated in deionized water. The resultant AuNRs were utilized without further purification for subsequent experiments.

Statistical Analysis

Statistical analyses were performed using Origin Pro 2018 and MATLAB R2013a software. The qualitative performance of the probe was assessed using linear discriminant analysis (LDA). Partial least squares regression (PLSR) was utilized as a powerful multivariate calibration method to quantify antioxidants and total antioxidants. Principal component analysis (PCA) was applied to reduce the dimensionality of the dataset when necessary. Model accuracy was estimated using leave-one-out cross-validation and test-set validation. The Jackknifed classification matrix and canonical score plots were applied to assess the classification model outcomes. Two-dimensional (2D) confidence ellipses indicating 95% confidence limits were plotted around cluster centroids to demonstrate the statistical significance of classifications. The MVC1 toolbox in MATLAB R2019b was used for PLSR analyses, determining analytical figures of merit such as the correlation coefficient (R^2), root-mean-square error of calibration (RMSEC), root-mean-square error of cross-validation (RMSECV), root-mean-square error of prediction (RMSEP), sensitivity (SEN), analytical sensitivity (Anal. SEN), limit of detection (LOD), and limit of quantification (LOQ).

LOD and LOQ Formulas:

In this study, the LOD for each antioxidant (AA, CYS, GSH, and UA) and total antioxidant capacity (TAC) was determined using the MVC1 toolbox in MATLAB, with the results presented systematically in Table 1. The formula used to define the LOD and limit of quantification (LOQ) for multivariate calibration is provided below:

$$\mathbf{LOD} = 3.3 [\mathbf{SEN}^{-2} \sigma_x^2 (1+\mathbf{h}_0) + \mathbf{h}_0 \sigma_{y, cal}^2]^{1/2}$$

where:

- SEN is the sensitivity,
- σ_x^2 is the instrumental signal variance,
- $\sigma_{y, cal}^2$ is the variance of the analyte concentration in the calibration set,
- h_0 is the leverage of the blank sample.

The factor 3.3 corresponds to a 5% error margin for Type I and II errors. The limit of quantification (LOQ) is defined as:

$$\mathbf{LOQ} = 10.0/3.3 \mathbf{LOD}$$

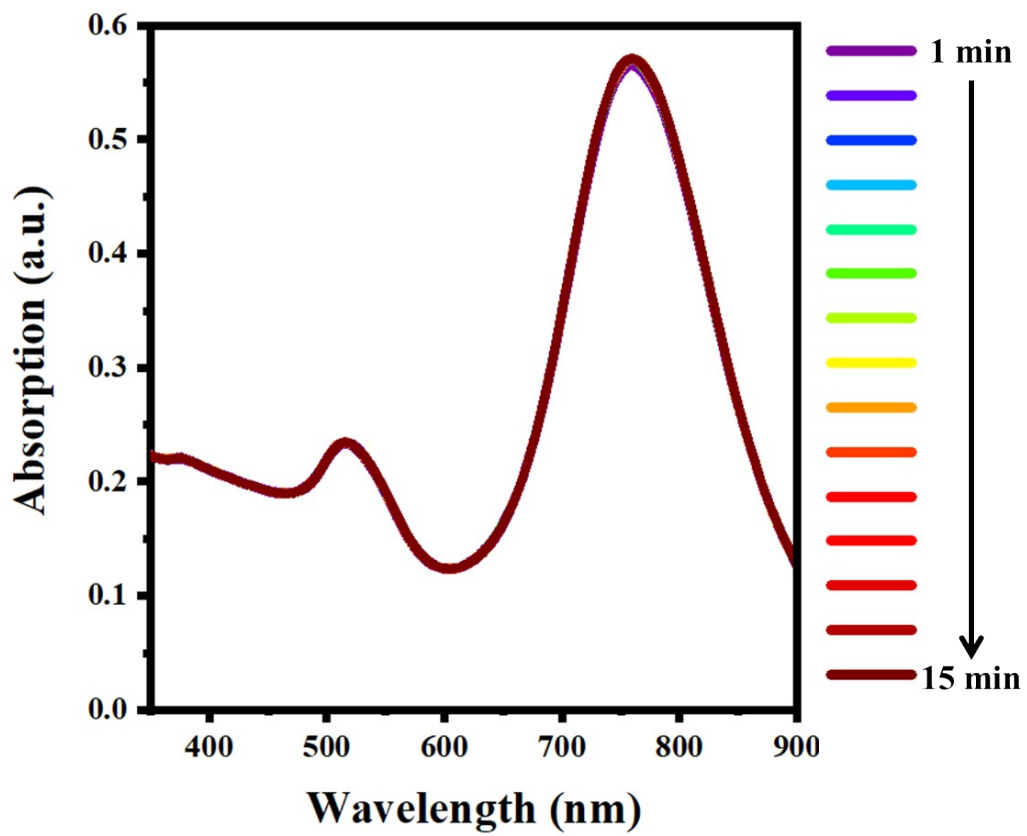


Fig. S1 Assessing the stability of AuNRs in pH 7 B.R. buffer: UV-vis spectra within 15 minutes.

Table S1. Comparative redox potentials for key antioxidants in the human body.

Redox Pair	Redox potential (volts)
Ascorbic acid oxidized/reduced	+0.08
Cystine/ Cysteine	-0.22
Glutathione oxidized/reduced	-0.24
Uric acid oxidized/reduced	0.35

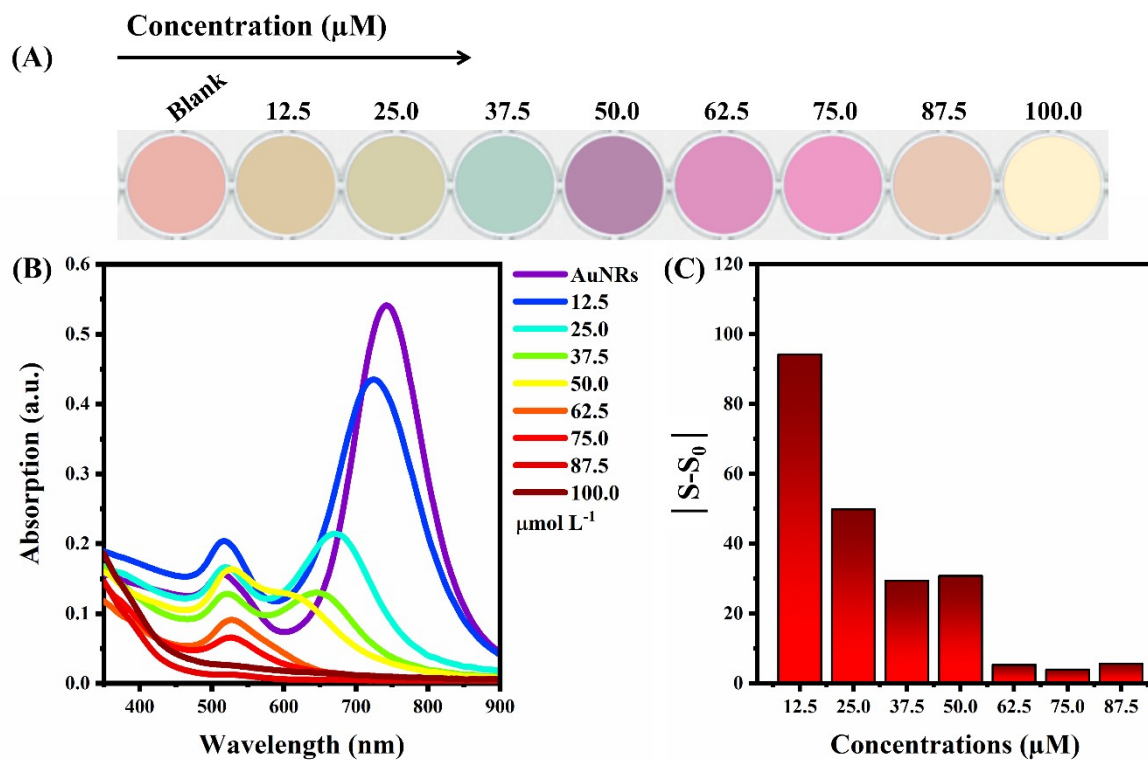


Fig. S2 Effect of NBS concentrations on the multi-colorimetric responses of AuNRs, (A) the corresponding images of the probe, (B) the absorption spectra of the proposed probe, and (C) the corresponding bar plot as a function of NBS concentration (pH 7 B.R. buffer) at 15 min in both incubation time and analysis time.

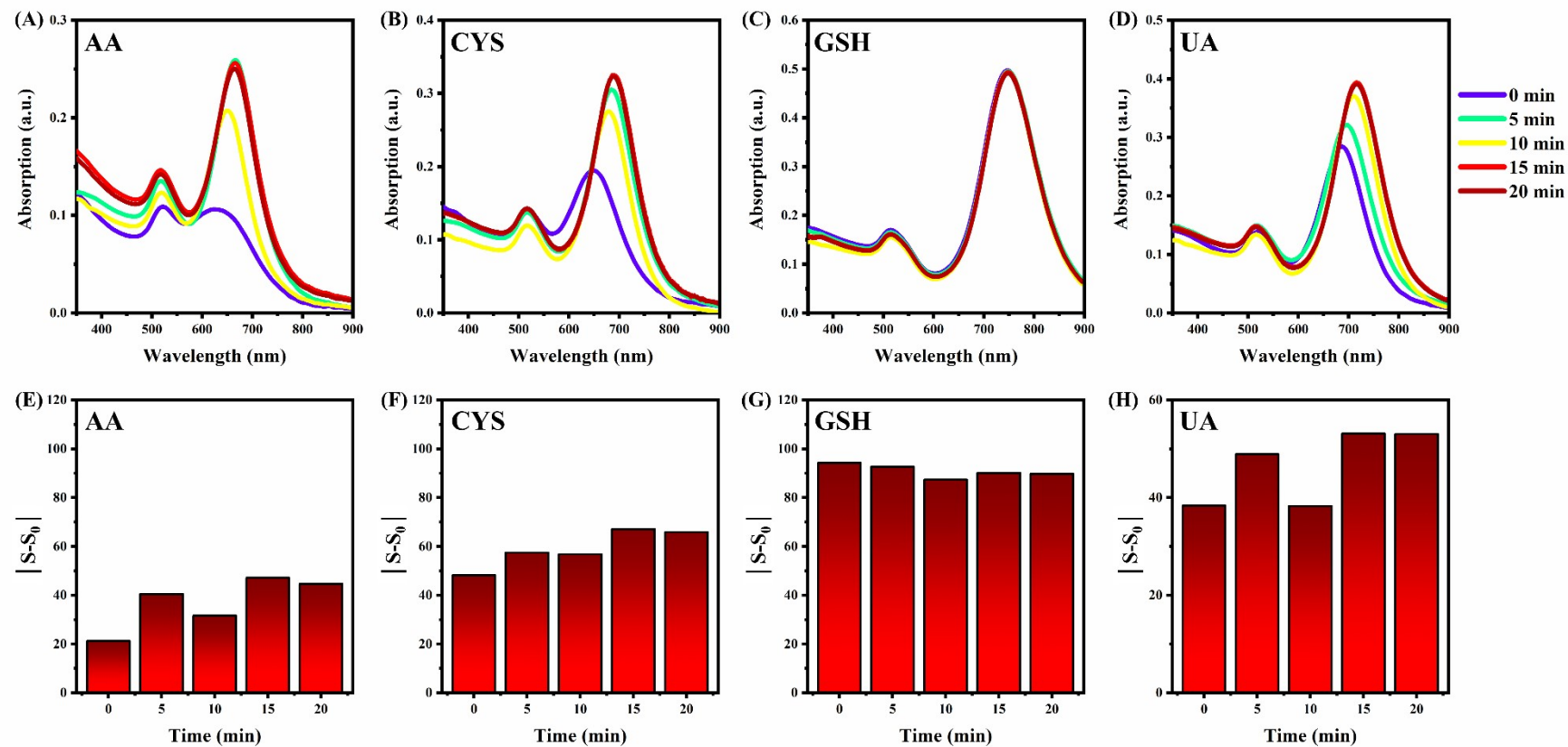


Fig. S3 Effect of incubation time on the multi-colorimetric responses of AuNRs, spectral variations of 10 μ M of each antioxidant, pH 7 B.R buffer, and analysis time 15 min (A) AA, (B) CYS, (C) GSH, and (D) UA, (E-H) bar plots representing variations of AuNRs spectra as a function of incubation time in the presence of AA, CYS, GSH, and UA respectively.

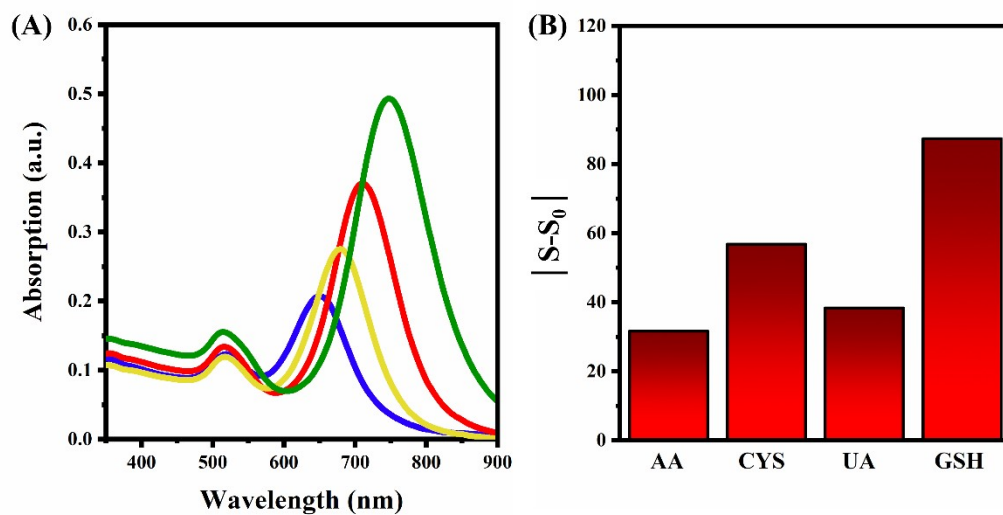


Fig. S4 UV-vis absorption profile of the proposed probe after 10-minute incubation with 75 μM NBS and 10 μM of individual antioxidants in pH 7 B.R. buffer.

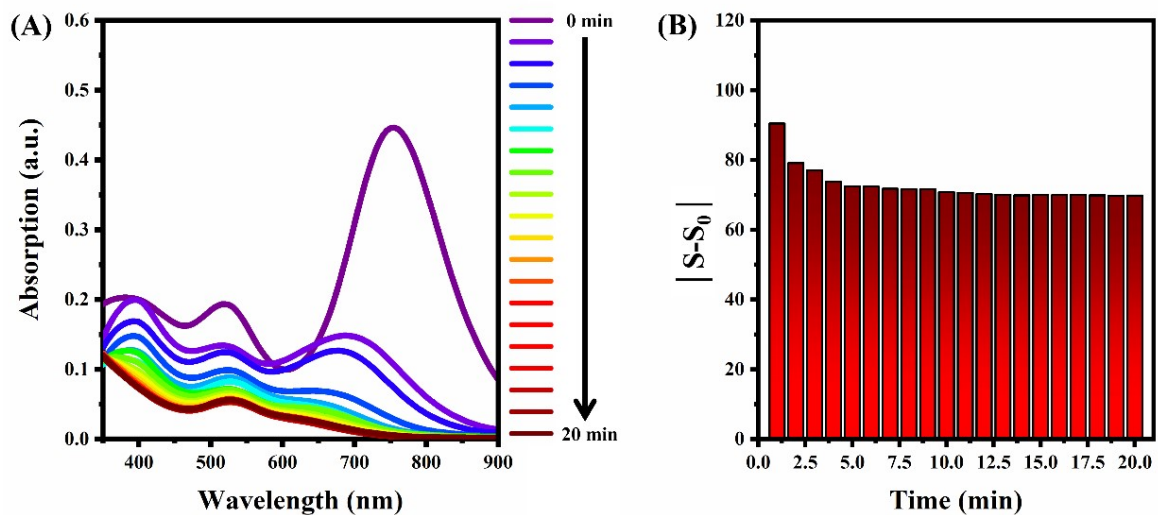


Fig. S5 Effect of time-course variation in absorption spectra of the AuNRs, (A) spectral variations, (B) bar plot representing variations of AuNRs spectra as a function of time-course variation in the presence of 75 μM NBS. The incubation time was 10 min.

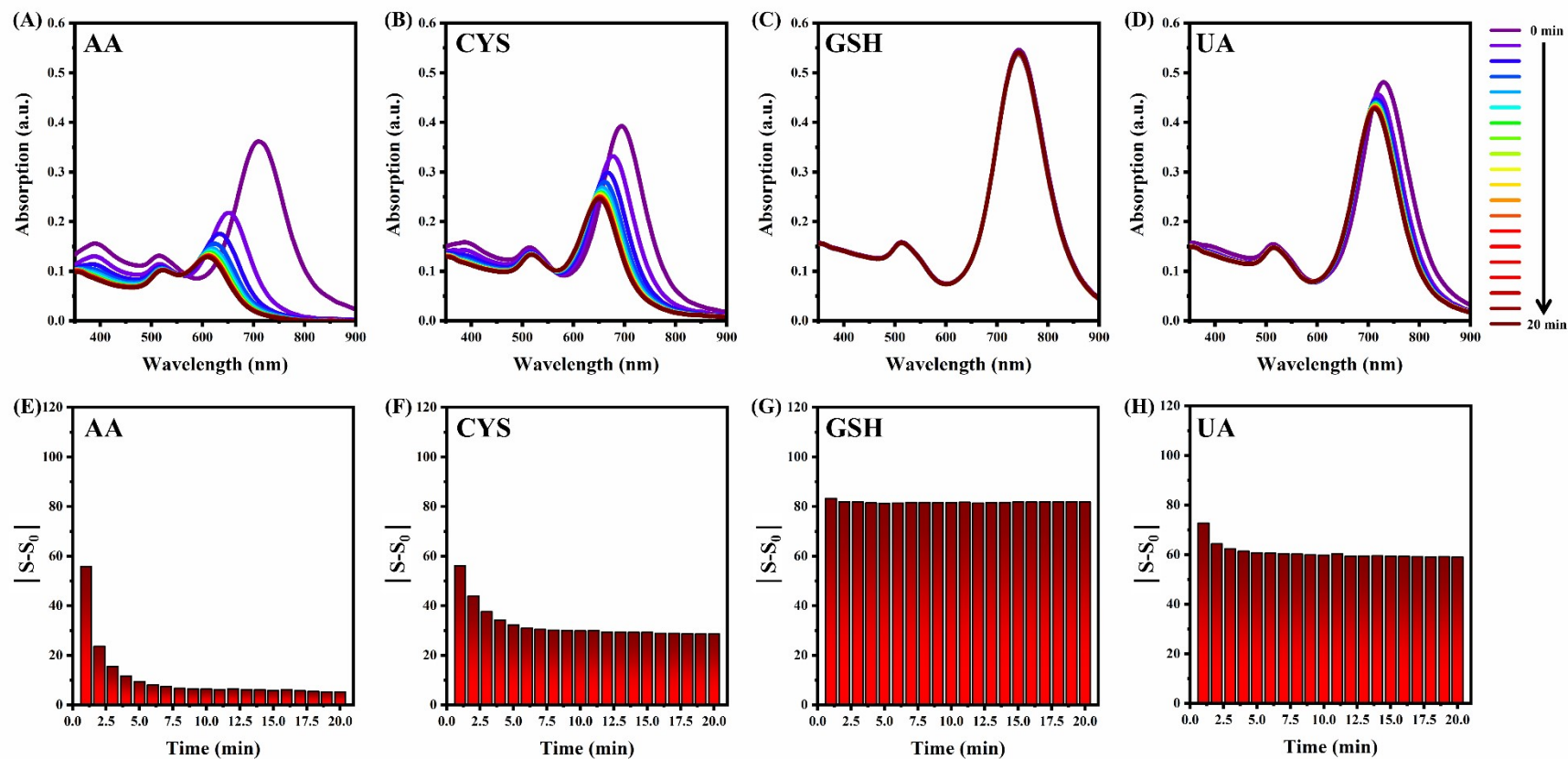


Fig. S6 Effect of time-course variation in absorption spectra of the AuNRs, spectral variations of (A) ASA, (B) CYS, (C) GSH, and (D) UA, (E-H) bar plots representing variations of AuNRs spectra as a function of time-course variation in the presence of AA, CYS, GSH, and UA, respectively. The concentration of NBS and each antioxidant was $75 \mu\text{mol L}^{-1}$ and $10 \mu\text{mol L}^{-1}$, respectively. The incubation time was 10 minutes in pH 7 B.R. buffer.

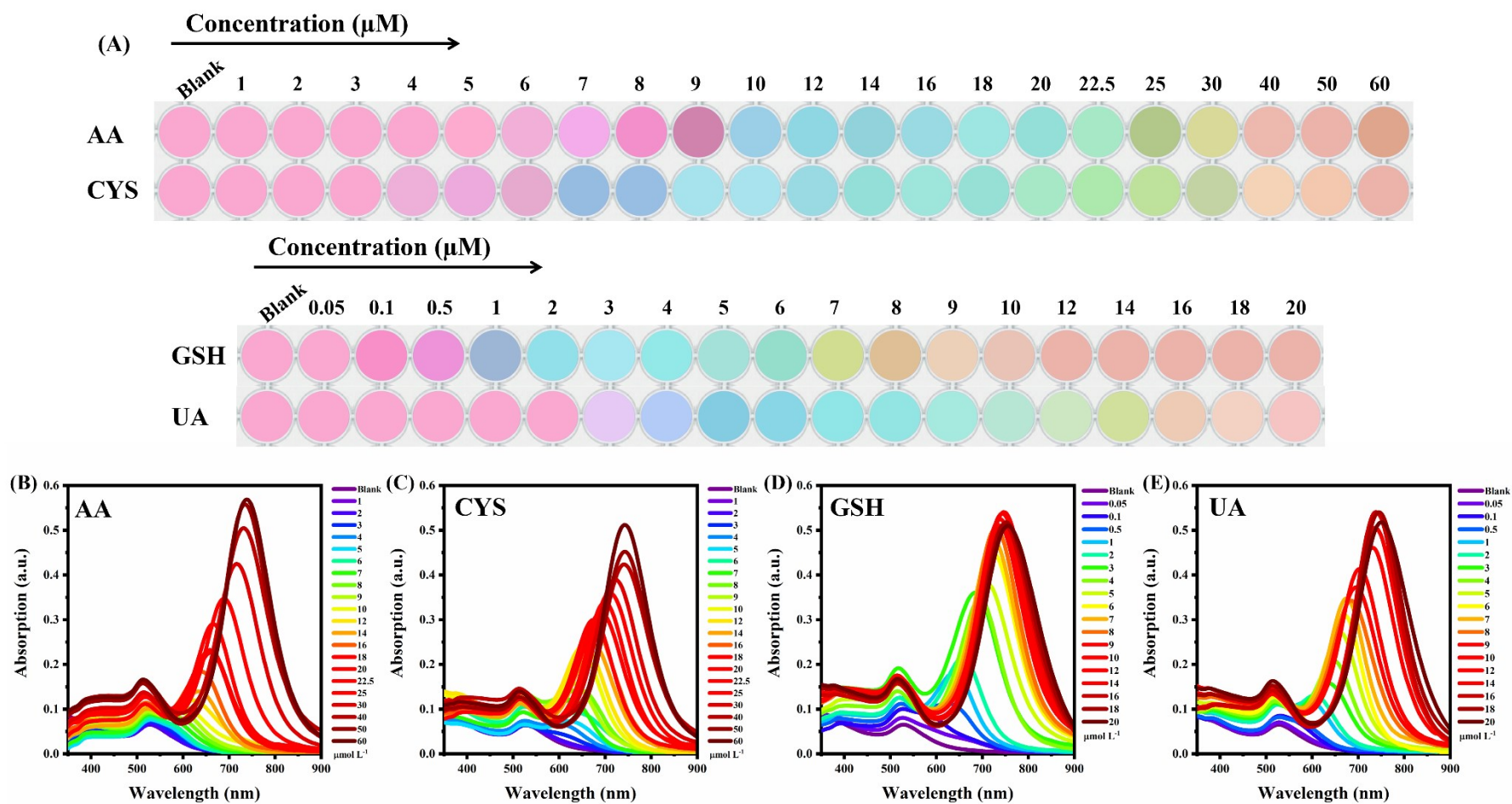


Fig. S7 (A) Color variation images and variation responses of the probe to different concentrations of (B) AA, (C) CYS, (D) GSH, and (E) UA.

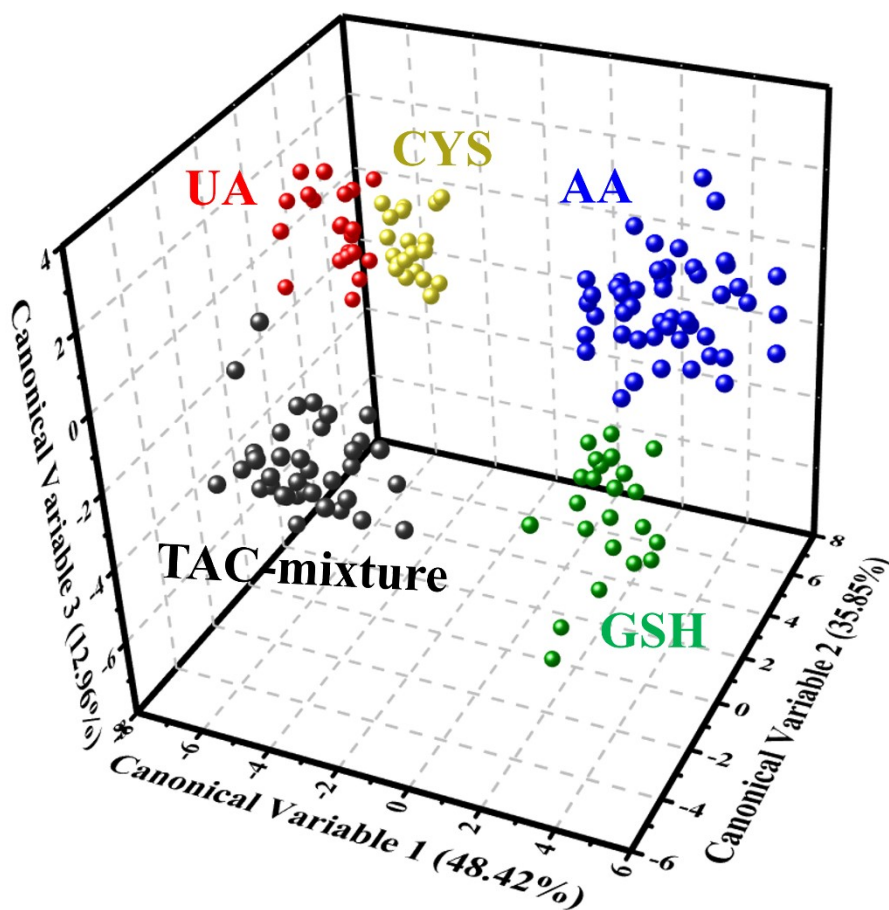


Fig. S8 3D LDA score plots for the discrimination of four classes of antioxidants (i.e., AA, CYS, GSH, and UA) and total antioxidants as a TAC-mixture.

Table S2. Jackknifed classification matrix for the discrimination of single-component samples (AA and CYS 1-60 $\mu\text{mol L}^{-1}$; UA and GSH 0.05-20 $\mu\text{mol L}^{-1}$) and TAC-mixture as a multicomponent (0.05-14 $\mu\text{mol L}^{-1}$) in their entire concentration range.

		<i>Predicted class</i>					<i>Total</i>	<i>Sensitivity (%)</i>	<i>Specificity (%)</i>	<i>Precision (%)</i>
		<i>AA</i>	<i>CYS</i>	<i>GSH</i>	<i>UA</i>	<i>TAC-mixture</i>				
<i>Nominal class</i>	<i>AA</i>	51	0	0	0	0	51	100.00	100.00	100.00
		100.00%	0.00%	0.00%	0.00%	0.00%	100.00%			
	<i>CYS</i>	0	21	0	0	0	21	100.00	100.00	100.00
		0.00%	100.00%	0.00%	0.00%	0.00%	100.00%			
	<i>GSH</i>	0	0	21	0	0	21	100.00	100.00	100.00
		0.00%	0.00%	100.00%	0.00%	0.00%	100.00%			
	<i>UA</i>	0	0	0	24	0	24	100.00	100.00	100.00
		0.00%	0.00%	0.00%	100.00%	0.00%	100.00%			
	<i>TAC-mixture</i>	0	0	0	0	36	36	100.00	100.00	100.00
		0.00%	0.00%	0.00%	0.00%	100.00%	100.00%			
<i>Total</i>	51	21	21	24	36	1153	100.00	100.00	100.00	
	33.33%	13.73%	13.73%	15.69%	23.53%	100.00%				

Table S4. Jackknifed classification matrix for the discrimination of CYS in the entire concentration range.

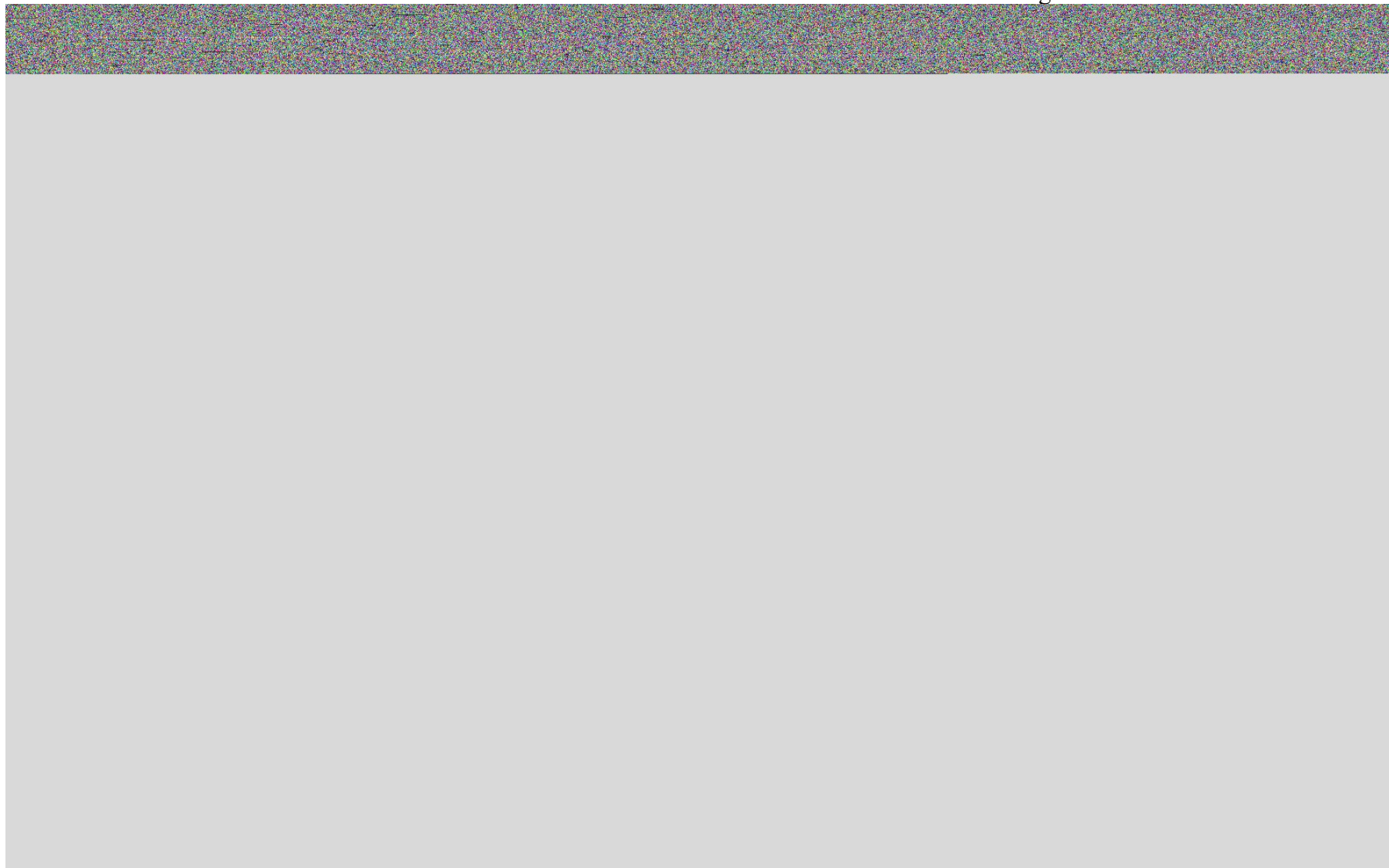


Table S5. Jackknifed classification matrix for the discrimination of GSH in the entire concentration range.

		Predicted class																		Sensitivity (%)	Specificity (%)	Precision(%)	
		0.05	0.1	0.5	1	2	3	4	5	6	7	8	9	10	12	14	16	18	20				Total
Nominal class	0.05	3	0	0	0	0	0	0	0	0	0	0	0	0	0	0	0	0	0	3	100.00	100.00	100.00
		100.00%	0.00%	0.00%	0.00%	0.00%	0.00%	0.00%	0.00%	0.00%	0.00%	0.00%	0.00%	0.00%	0.00%	0.00%	0.00%	0.00%	0.00%	7.41%			
	0.1	0	3	0	0	0	0	0	0	0	0	0	0	0	0	0	0	0	0	3	100.00	100.00	100.00
		0.00%	100.00%	0.00%	0.00%	0.00%	0.00%	0.00%	0.00%	0.00%	0.00%	0.00%	0.00%	0.00%	0.00%	0.00%	0.00%	0.00%	0.00%	7.41%			
	0.5	0	0	3	0	0	0	0	0	0	0	0	0	0	0	0	0	0	0	3	100.00	100.00	100.00
		0.00%	0.00%	100.00%	0.00%	0.00%	0.00%	0.00%	0.00%	0.00%	0.00%	0.00%	0.00%	0.00%	0.00%	0.00%	0.00%	0.00%	0.00%	7.41%			
	1	0	0	0	3	0	0	0	0	0	0	0	0	0	0	0	0	0	0	3	100.00	100.00	100.00
		0.00%	0.00%	0.00%	100.00%	0.00%	0.00%	0.00%	0.00%	0.00%	0.00%	0.00%	0.00%	0.00%	0.00%	0.00%	0.00%	0.00%	0.00%	7.41%			
	2	0	0	0	0	3	0	0	0	0	0	0	0	0	0	0	0	0	0	3	100.00	100.00	100.00
		0.00%	0.00%	0.00%	0.00%	100.00%	0.00%	0.00%	0.00%	0.00%	0.00%	0.00%	0.00%	0.00%	0.00%	0.00%	0.00%	0.00%	0.00%	7.41%			
	3	0	0	0	0	0	3	0	0	0	0	0	0	0	0	0	0	0	0	3	100.00	100.00	100.00
		0.00%	0.00%	0.00%	0.00%	0.00%	100.00%	0.00%	0.00%	0.00%	0.00%	0.00%	0.00%	0.00%	0.00%	0.00%	0.00%	0.00%	0.00%	7.41%			
	4	0	0	0	0	0	0	3	0	0	0	0	0	0	0	0	0	0	0	3	100.00	100.00	100.00
		0.00%	0.00%	0.00%	0.00%	0.00%	0.00%	100.00%	0.00%	0.00%	0.00%	0.00%	0.00%	0.00%	0.00%	0.00%	0.00%	0.00%	0.00%	7.41%			
	5	0	0	0	0	0	0	0	3	0	0	0	0	0	0	0	0	0	0	3	100.00	100.00	100.00
		0.00%	0.00%	0.00%	0.00%	0.00%	0.00%	0.00%	100.00%	0.00%	0.00%	0.00%	0.00%	0.00%	0.00%	0.00%	0.00%	0.00%	0.00%	7.41%			
	6	0	0	0	0	0	0	0	0	3	0	0	0	0	0	0	0	0	0	3	100.00	100.00	100.00
		0.00%	0.00%	0.00%	0.00%	0.00%	0.00%	0.00%	0.00%	100.00%	0.00%	0.00%	0.00%	0.00%	0.00%	0.00%	0.00%	0.00%	0.00%	7.41%			
	7	0	0	0	0	0	0	0	0	0	3	0	0	0	0	0	0	0	0	3	100.00	100.00	100.00
		0.00%	0.00%	0.00%	0.00%	0.00%	0.00%	0.00%	0.00%	0.00%	100.00%	0.00%	0.00%	0.00%	0.00%	0.00%	0.00%	0.00%	0.00%	7.41%			
8	0	0	0	0	0	0	0	0	0	0	3	0	0	0	0	0	0	0	3	100.00	100.00	100.00	
	0.00%	0.00%	0.00%	0.00%	0.00%	0.00%	0.00%	0.00%	0.00%	0.00%	100.00%	0.00%	0.00%	0.00%	0.00%	0.00%	0.00%	0.00%	7.41%				
9	0	0	0	0	0	0	0	0	0	0	0	3	0	0	0	0	0	0	3	100.00	100.00	100.00	
	0.00%	0.00%	0.00%	0.00%	0.00%	0.00%	0.00%	0.00%	0.00%	0.00%	0.00%	100.00%	0.00%	0.00%	0.00%	0.00%	0.00%	0.00%	7.41%				
10	0	0	0	0	0	0	0	0	0	0	0	0	3	0	0	0	0	0	3	100.00	100.00	100.00	
	0.00%	0.00%	0.00%	0.00%	0.00%	0.00%	0.00%	0.00%	0.00%	0.00%	0.00%	0.00%	100.00%	0.00%	0.00%	0.00%	0.00%	0.00%	7.41%				
12	0	0	0	0	0	0	0	0	0	0	0	0	0	3	0	0	0	0	3	100.00	100.00	100.00	
	0.00%	0.00%	0.00%	0.00%	0.00%	0.00%	0.00%	0.00%	0.00%	0.00%	0.00%	0.00%	0.00%	100.00%	0.00%	0.00%	0.00%	0.00%	7.41%				
14	0	0	0	0	0	0	0	0	0	0	0	0	0	0	3	0	0	0	3	100.00	100.00	100.00	
	0.00%	0.00%	0.00%	0.00%	0.00%	0.00%	0.00%	0.00%	0.00%	0.00%	0.00%	0.00%	0.00%	0.00%	100.00%	0.00%	0.00%	0.00%	7.41%				
16	0	0	0	0	0	0	0	0	0	0	0	0	0	0	0	3	0	0	3	100.00	100.00	100.00	
	0.00%	0.00%	0.00%	0.00%	0.00%	0.00%	0.00%	0.00%	0.00%	0.00%	0.00%	0.00%	0.00%	0.00%	0.00%	100.00%	0.00%	0.00%	7.41%				
18	0	0	0	0	0	0	0	0	0	0	0	0	0	0	0	0	3	0	3	100.00	100.00	100.00	
	0.00%	0.00%	0.00%	0.00%	0.00%	0.00%	0.00%	0.00%	0.00%	0.00%	0.00%	0.00%	0.00%	0.00%	0.00%	0.00%	100.00%	0.00%	7.41%				
20	0	0	0	0	0	0	0	0	0	0	0	0	0	0	0	0	0	3	3	100.00	100.00	100.00	
	0.00%	0.00%	0.00%	0.00%	0.00%	0.00%	0.00%	0.00%	0.00%	0.00%	0.00%	0.00%	0.00%	0.00%	0.00%	0.00%	0.00%	100.00%	7.41%				
Total	3	3	3	3	3	3	3	3	3	3	3	3	3	3	3	3	3	3	54	100.00	100.00	100.00	
	7.41%	7.41%	7.41%	7.41%	7.41%	7.41%	7.41%	7.41%	7.41%	7.41%	7.41%	7.41%	7.41%	7.41%	7.41%	7.41%	7.41%	7.41%	100.00%				

Table S6. Jackknifed classification matrix for the discrimination of UA in the entire concentration range.

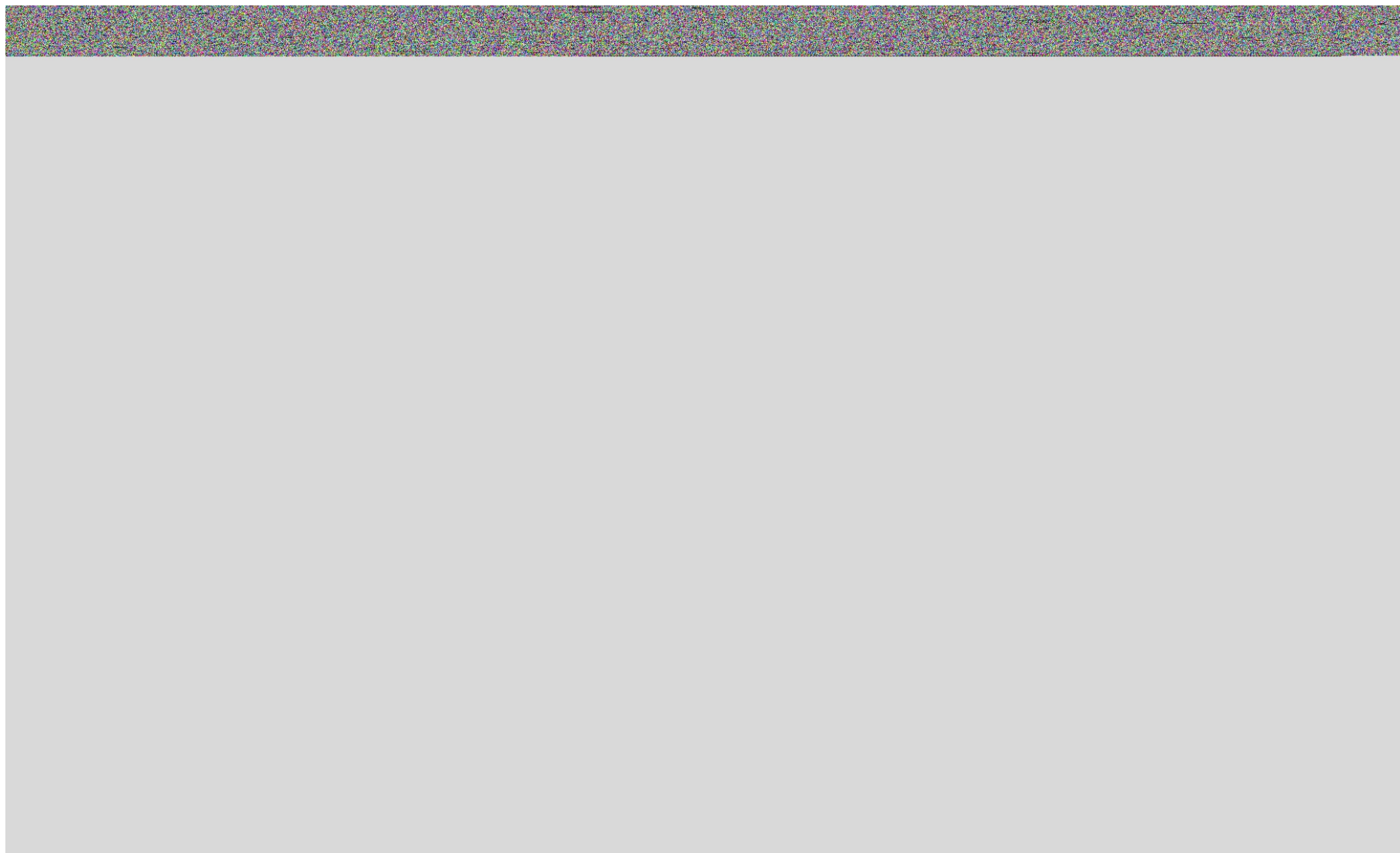
The table content is completely obscured by a large, solid gray rectangular area. Only the top header row is visible, showing a dense, multi-colored pattern of small characters, likely representing the column headers of the classification matrix.

Table S7. Jackknifed classification matrix for the discrimination of TAC-mixture in the entire concentration range.

		Predicted class															Sensitivity (%)	Specificity (%)	Precision(%)	
		0.05	0.1	0.5	1	2	3	4	5	6	7	8	9	10	12	14				Total
Nominal class	0.05	3	0	0	0	0	0	0	0	0	0	0	0	0	0	0	3	100.00	100.00	100.00
		100.00%	0.00%	0.00%	0.00%	0.00%	0.00%	0.00%	0.00%	0.00%	0.00%	0.00%	0.00%	0.00%	0.00%	0.00%	6.67%			
	0.1	0	3	0	0	0	0	0	0	0	0	0	0	0	0	0	3	100.00	100.00	100.00
		0.00%	100.00%	0.00%	0.00%	0.00%	0.00%	0.00%	0.00%	0.00%	0.00%	0.00%	0.00%	0.00%	0.00%	0.00%	6.67%			
	0.5	0	0	3	0	0	0	0	0	0	0	0	0	0	0	0	3	100.00	100.00	100.00
		0.00%	0.00%	100.00%	0.00%	0.00%	0.00%	0.00%	0.00%	0.00%	0.00%	0.00%	0.00%	0.00%	0.00%	0.00%	6.67%			
	1	0	0	0	3	0	0	0	0	0	0	0	0	0	0	0	3	100.00	100.00	100.00
		0.00%	0.00%	0.00%	100.00%	0.00%	0.00%	0.00%	0.00%	0.00%	0.00%	0.00%	0.00%	0.00%	0.00%	0.00%	6.67%			
	2	0	0	0	0	3	0	0	0	0	0	0	0	0	0	0	3	100.00	100.00	100.00
		0.00%	0.00%	0.00%	0.00%	100.00%	0.00%	0.00%	0.00%	0.00%	0.00%	0.00%	0.00%	0.00%	0.00%	0.00%	6.67%			
	3	0	0	0	0	0	3	0	0	0	0	0	0	0	0	0	3	100.00	100.00	100.00
		0.00%	0.00%	0.00%	0.00%	0.00%	100.00%	0.00%	0.00%	0.00%	0.00%	0.00%	0.00%	0.00%	0.00%	0.00%	6.67%			
	4	0	0	0	0	0	0	3	0	0	0	0	0	0	0	0	3	100.00	100.00	100.00
		0.00%	0.00%	0.00%	0.00%	0.00%	0.00%	100.00%	0.00%	0.00%	0.00%	0.00%	0.00%	0.00%	0.00%	0.00%	6.67%			
	5	0	0	0	0	0	0	0	3	0	0	0	0	0	0	0	3	100.00	100.00	100.00
		0.00%	0.00%	0.00%	0.00%	0.00%	0.00%	0.00%	100.00%	0.00%	0.00%	0.00%	0.00%	0.00%	0.00%	0.00%	6.67%			
	6	0	0	0	0	0	0	0	0	3	0	0	0	0	0	0	3	100.00	100.00	100.00
		0.00%	0.00%	0.00%	0.00%	0.00%	0.00%	0.00%	0.00%	100.00%	0.00%	0.00%	0.00%	0.00%	0.00%	0.00%	6.67%			
	7	0	0	0	0	0	0	0	0	0	3	0	0	0	0	0	3	100.00	100.00	100.00
		0.00%	0.00%	0.00%	0.00%	0.00%	0.00%	0.00%	0.00%	0.00%	100.00%	0.00%	0.00%	0.00%	0.00%	0.00%	6.67%			
8	0	0	0	0	0	0	0	0	0	0	3	0	0	0	0	3	100.00	100.00	100.00	
	0.00%	0.00%	0.00%	0.00%	0.00%	0.00%	0.00%	0.00%	0.00%	0.00%	100.00%	0.00%	0.00%	0.00%	0.00%	6.67%				
9	0	0	0	0	0	0	0	0	0	0	0	3	0	0	0	3	100.00	100.00	100.00	
	0.00%	0.00%	0.00%	0.00%	0.00%	0.00%	0.00%	0.00%	0.00%	0.00%	0.00%	100.00%	0.00%	0.00%	0.00%	6.67%				
10	0	0	0	0	0	0	0	0	0	0	0	0	3	0	0	3	100.00	100.00	100.00	
	0.00%	0.00%	0.00%	0.00%	0.00%	0.00%	0.00%	0.00%	0.00%	0.00%	0.00%	0.00%	100.00%	0.00%	0.00%	6.67%				
12	0	0	0	0	0	0	0	0	0	0	0	0	0	3	0	3	100.00	100.00	100.00	
	0.00%	0.00%	0.00%	0.00%	0.00%	0.00%	0.00%	0.00%	0.00%	0.00%	0.00%	0.00%	0.00%	100.00%	0.00%	6.67%				
14	0	0	0	0	0	0	0	0	0	0	0	0	0	0	3	3	100.00	100.00	100.00	
	0.00%	0.00%	0.00%	0.00%	0.00%	0.00%	0.00%	0.00%	0.00%	0.00%	0.00%	0.00%	0.00%	0.00%	100.00%	6.67%				
Total	3	3	3	3	3	3	3	3	3	3	3	3	3	3	3	45	100.00	100.00	100.00	
	6.67%	6.67%	6.67%	6.67%	6.67%	6.67%	6.67%	6.67%	6.67%	6.67%	6.67%	6.67%	6.67%	6.67%	6.67%	100.00%				

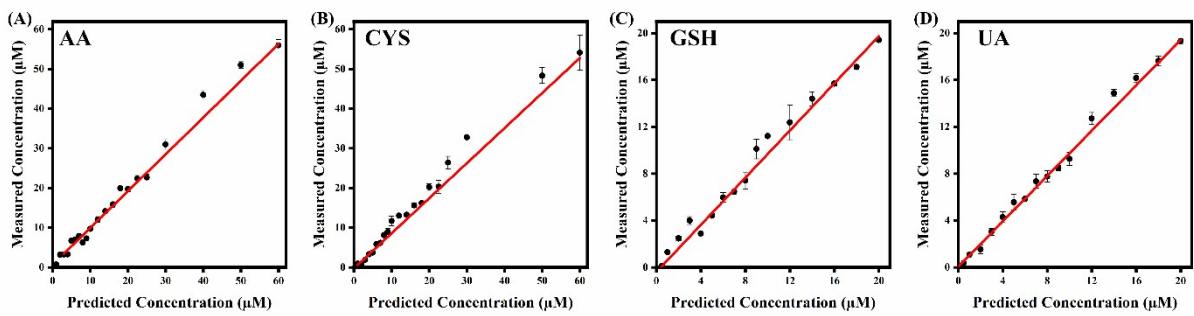


Fig. S9 Predicted vs measured concentration plots with PLSR for (A) AA, (B) CYS, (C) GSH, (D) and UA.

Table S8. Comparison of the proposed method with other reported methods for detection of antioxidants.

Analytes	Materials	Detection method	Linear range ($\mu\text{mol L}^{-1}$)	LOD ($\mu\text{mol L}^{-1}$)	References
AA CYS GSH	Iron-doped carbon nitride	Smartphone-based colorimetric	50-1000 5-22.5 5-30	30 4 8	1
AA CYS GSH	Ag-MOF	Visual-based	3-40	0.048 0.050 0.088	3
TAC	SMOF nanozyme	Colorimetric	50–700	33.4	4
AA CYS GSH	Mn-MOF peroxidase-like nanozymes	Temperature-resilient	3.0-25 3.0–33 3.0-35	0.040 0.047 0.067	5
TAC	Au-doped g-C ₃ N ₄ nanosheet	Colorimetric	Not reported	1.0	6
AA	Nitrogen-Doped Carbon Nanoflowers	Colorimetric	1.0–20.0	0.94	7
GSH CYS GA CA	Au ₂ Pt nanozymes	Colorimetric sensor array	4–20 0-16 1-20 2-12	0.124 0.1163 0.2570 0.1885	8
AA CYS GSH UA TAC	Anti-etching of AuNRs	Colorimetric	3.1-60.0 2.6-60.0 1.2-20.0 0.8-14.0 0.7-14.0	1.1 0.9 0.4 0.3 0.2	This Work

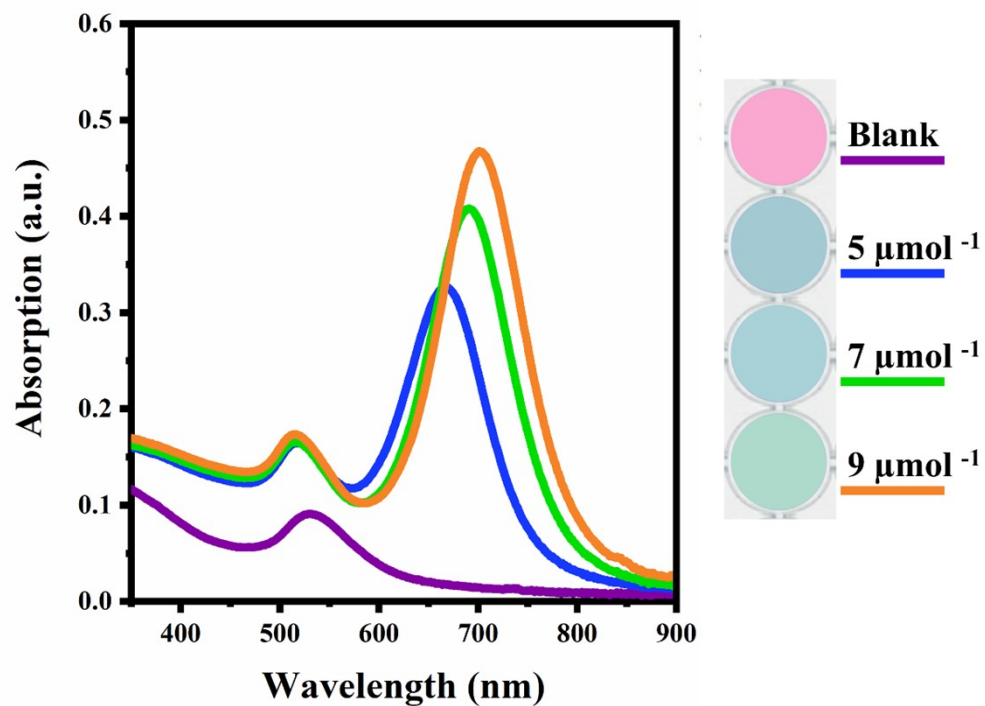


Fig. S10 UV-vis spectra and corresponding color photographs of three different TAC unknown in total concentration of 5, 7, and 9 $\mu\text{mol L}^{-1}$ in human saliva sample.

Table S9. LDA posterior probability outcomes for identifying TAC unknown samples in human saliva. All 9 samples were given as a test set to the pre-trained LDA model of AA, CYS, GSH, UA, and TAC-mixture.

<i>Alleged</i>	<i>Post probabilities</i>					<i>Allocated</i>
	<i>AA</i>	<i>CYS</i>	<i>GSH</i>	<i>UA</i>	<i>TAC-mixture</i>	
TAC-mixture	5.44E-14	3.24E-18	4.75E-20	9.29E-18	1	TAC-mixture
TAC-mixture	1.83E-12	3.84E-9	9.72E-15	5.54E-7	1	TAC-mixture
TAC-mixture	2.90E-13	4.43E-10	1.33E-15	1.53E-8	1	TAC-mixture
TAC-mixture	2.50E-13	4.99E-27	2.36E-16	7.11E-28	1	TAC-mixture
TAC-mixture	2.92E-13	2.63E-38	8.17E-19	1.89E-42	1	TAC-mixture
TAC-mixture	3.36E-13	2.52E-23	9.71E-16	1.72E-23	1	TAC-mixture
TAC-mixture	1.82E-7	2.85E-4	0.04335	1.78E-4	0.95619	TAC-mixture
TAC-mixture	7.97E-21	1.34E-27	3.85E-15	2.03E-32	1	TAC-mixture
TAC-mixture	1.25E-10	1.23E-8	2.60E-6	1.64E-10	1	TAC-mixture

Table S10. LDA posterior probability outcomes for identifying TAC unknown samples in human saliva. All 9 samples were given as a test set to the pre-trained LDA model of TAC-mixture within the total concentration range of 0.05–14 $\mu\text{mol L}^{-1}$.

<i>Alleged</i>	<i>Post probabilities</i>															<i>Allocated</i>
	<i>0.05</i>	<i>0.1</i>	<i>0.5</i>	<i>1</i>	<i>2</i>	<i>3</i>	<i>4</i>	<i>5</i>	<i>6</i>	<i>7</i>	<i>8</i>	<i>9</i>	<i>10</i>	<i>12</i>	<i>14</i>	
5	0	0	0	0	0	0	0	1	3.39E-92	1.65E-58	0	0	0	0	0	5
5	0	0	0	0	0	0	0	1	0	0	0	0	0	0	0	5
5	0	0	0	0	0	0	0	1	0	1.82E-75	0	0	0	0	0	5
7	0	0	0	0	0	0	0	1.02E-179	3.76E-73	1	6.43E-127	4.65E-82	0	0	0	7
7	0	0	0	0	0	0	0	1.13E-153	8.36E-64	1	1.44E-145	1.20E-111	0	0	0	7
7	0	0	0	0	0	0	0	1.42E-136	2.18E-53	1	7.02E-139	9.23E-117	0	0	0	7
9	0	0	0	0	0	0	0	0	3.58E-265	1.18E-195	1.80E-80	1	0	0	0	9
9	0	0	0	0	0	0	0	0	9.28E-234	7.21E-165	3.29E-77	1	0	0	0	9
9	0	0	0	0	0	0	0	0	3.96E-246	2.83E-178	2.72E-77	1	0	0	0	9

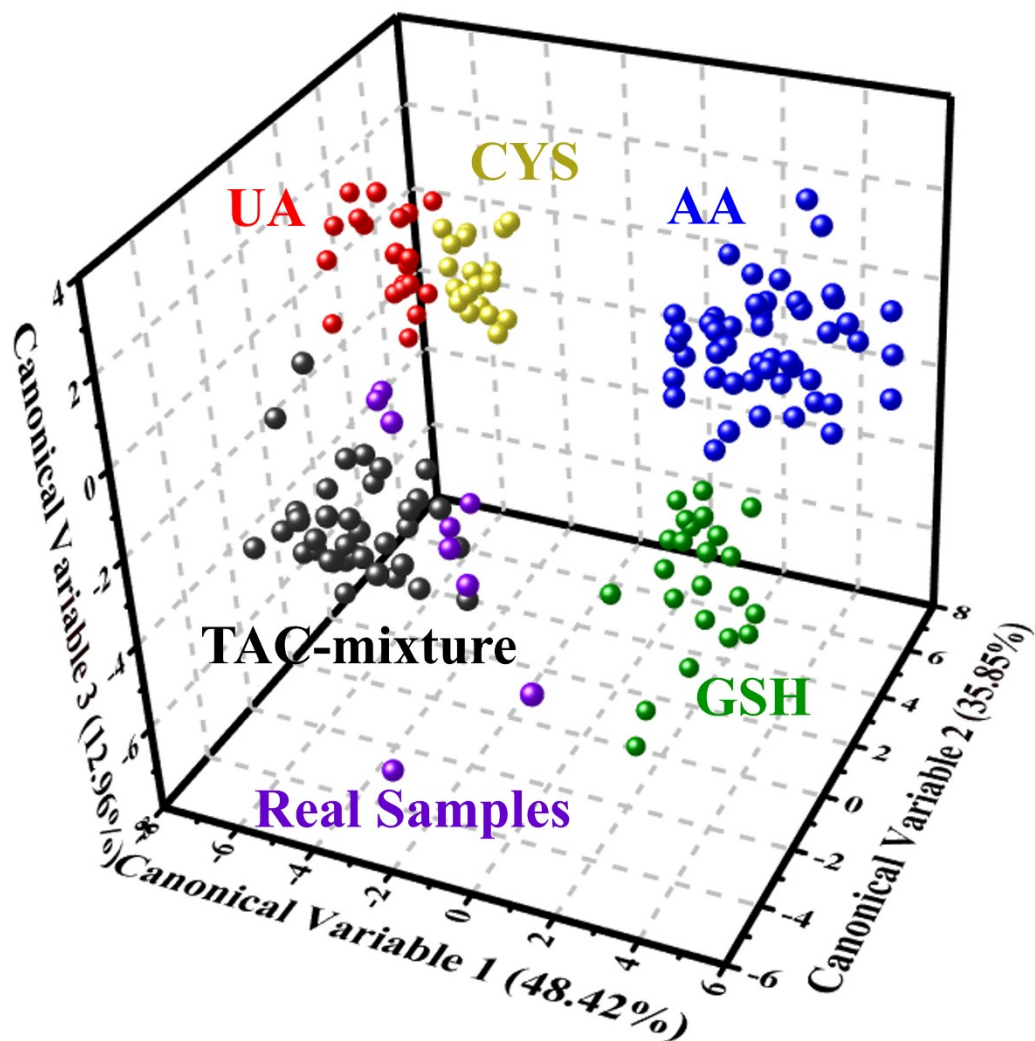


Fig. S11 3D LDA score plots for the discrimination of TAC unknown of real human saliva samples after combining the test set (real samples) with the pre-trained LDA model of AA, CYS, GSH, UA, and TAC-mixture. The saliva samples were spiked with three concentrations of total antioxidant.

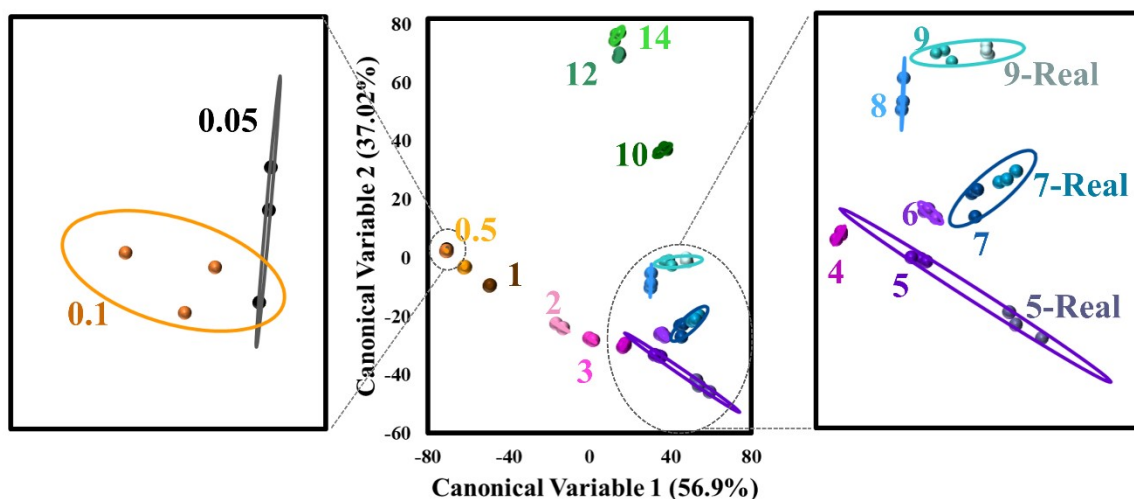


Fig. S12 2D LDA score plots for the discrimination of TAC unknown of real human saliva samples after combining the test set (real samples) with the pre-trained LDA model of TAC-mixture within the total concentration range of 0.05–14 $\mu\text{mol L}^{-1}$. The saliva samples were spiked with three concentrations of total antioxidants.

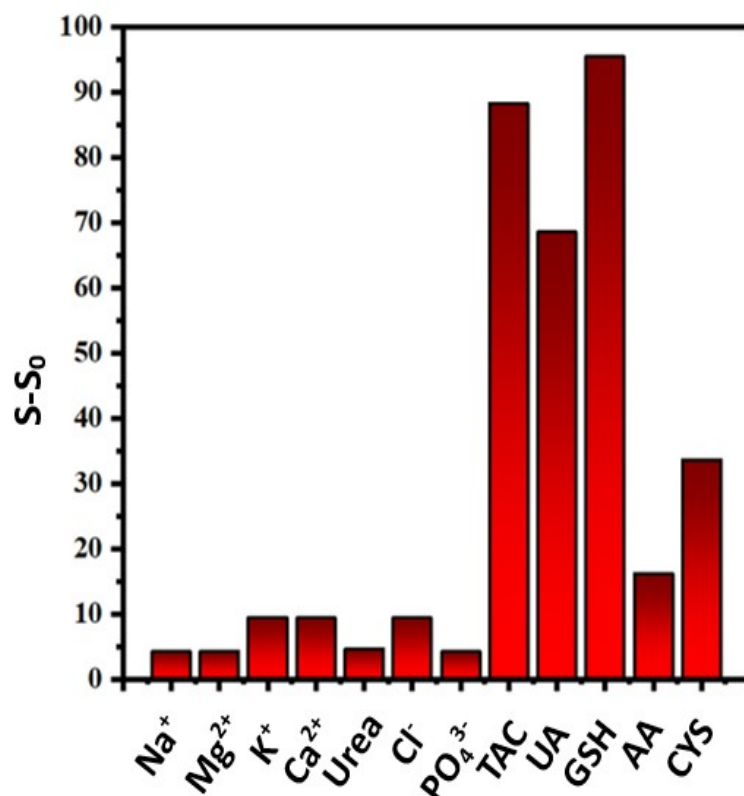


Fig. S13 Interference effect on the responses of the proposed probe ($[AA] = [CYS] = [GSH] = [UA] = [TAC] = 10 \mu\text{M}$, $[Urea] = 475 \mu\text{M}$, $([Na^+] = 1000 \mu\text{M}$, $[Ca^{2+}] = [K^+] = 500 \mu\text{M}$, $[Mg^{2+}] = 650 \mu\text{M}$) ($[Cl^-] = 650\mu\text{M}$, $[PO_4^{3-}] = 375 \mu\text{M}$).

References

1. M. R. Hormozi-Nezhad, H. Robotjazi and M. Jalali-Heravi, *Anal. Chim. Acta*, 2013, **779**, 14-21.
2. Y. Miao, M. Xia, C. Tao, J. Zhang, P. Ni, Y. Jiang and Y. Lu, *Talanta*, 2024, **267**, 125141.
3. S. S. Mohammed Ameen and K. M. Omer, *ACS Appl. Nano Mater.* 2024, **7**, 20793-20803.
4. H. Wu, J. Chen, P. Lin, Y. Su, H. Li, W. Xiao and J. Peng, *ACS Appl. Mater. Interfaces.* 2024, **16**, 39857-39866.
5. S. S. M. Ameen and K. M. Omer, *Food Chem.* 2024, **448**, 139170.
6. X. Li, W. Fan, H. Tang, D. Li, Y. Xiao, B. Yang, Y. Zhao and P. Wu, *Food Chem.* 2024, **439**, 138158.
7. Y.-W. Mao, J.-Q. Li, R. Zhang, A.-J. Wang and J.-J. Feng, *ACS Appl. Nano Mater.* 2023, **6**, 2805-2812.
8. F. Wu, H. Wang, J. Lv, X. Shi, L. Wu and X. Niu, *Biosens. Bioelectron.* 2023, **236**, 115417.